# Experimental Investigation on Traction, Mobility, and Energy Usage of a Tracked Autonomous Ground Vehicle on a Sloped Soil Bin

Article · June 2022

DOI: 10.13031/ja.14860

4 authors:

Chetan Badgujar
Kansas State University
16 PUBLICATIONS   32 CITATIONS

Daniel Flippo
Kansas State University
30 PUBLICATIONS   102 CITATIONS

Edwin Brokesh
Kansas State University
11 PUBLICATIONS   33 CITATIONS

Stephen Welch
Kansas State University
129 PUBLICATIONS   3,719 CITATIONS

Some of the authors of this publication are also working on these related projects:

Project   Biomass harvesting costs View project

Project   Non-invasive measurement View project

# EXPERIMENTAL INVESTIGATION ON TRACTION, MOBILITY AND ENERGY USAGE OF A TRACKED AUTONOMOUS GROUND VEHICLE ON A SLOPED SOIL BIN

Chetan M. Badgujar[1,*],   Daniel Flippo[1],   Edwin Brokesh[1],   Stephen Welch[1]

1 Biological and Agricultural Engineering,   Kansas State University,   Manhattan,   United States.

* Correspondence: chetan19@ksu.edu

## Highlights

- Laying the groundwork for AGV mobility models for high slope terrain operations.
- AGV drawbar pull performance was evaluated on a level terrain, uphill and downhill slopes up to 18˚ on a soil bin.
- AGV generates the optimum power efficiency with enough drawbar pull to perform a range of agricultural operations on uphill and downhill slopes up to 18˚.
- The study explored the suitability and established the boundary conditions of small size ground vehicles on the high slope farming.
- Generated sloped traction data would empower the multi-AGV system on sloped terrain.

**Abstract.** *Excessive steepness of grasslands, hills, or uneven terrain presents difficulties for farming with large conventional equipment. Therefore, a fleet of Autonomous Ground Vehicles (AGV) is proposed to perform primary agricultural operations on high sloped hills or terrain. However, it is imperative to understand how an individual AGV functions on sloping terrain under varying load and speed. Hence, this study aims to investigate the traction, mobility, and energy consumption characteristics of AGV on a sloped soil bin environment. A drawbar pull performance of the prototype AGV was evaluated on a level terrain and variable slope of 10˚ and 18˚, both uphill and downhill, at varying drawbar pull (P) and AGV speed. The AGV's performance metrics include power efficiency (PE), travel reduction (TR), and power number (PN) which relates to AGV's traction, mobility, and energy usage, respectively. The AGV generated drawbar pull equivalent to its weight only on downhill run for reduced PE. On a level terrain (0˚), the peak PE was 0.20 and was found to be 108.3% and 328.6% higher on 10˚ and 18˚ downhill run than uphill with 55.5% and 133% increase in drawbar pull, respectively. Both applied drawbar pull and*

*uphill operation caused the AGV's TR. The TR, corresponding to a peak PE, increased from 10% to 30%, respectively, on 0˚ and both 10˚ and 18˚ uphill. The optimum values of power number ranged from 2 to 4. The AGV delivers the optimum PE and generates enough drawbar pull with an optimum TR to perform a range of agricultural operations on a slope up to 18˚. This study explored the suitability and established the boundary conditions of small size ground vehicles for high-sloped farming. Besides this, the study also aims to generate an AGV's slope traction database to optimize its control variables, design optimization, and develop a mobility model for sloped terrain.*

*Keywords. Power efficiency, travel reduction, drawbar pull, ground vehicle, Multi-AGV fleet, slope.*

## INTRODUCTION

Approximately 97% of our food comes from arable land (Costanza *et al*., 2015), but arable land expansion remains a critical factor in food production growth to feed continuously burgeoning population. An additional minimum of 100 million ha of agricultural land use is needed by 2050 to meet the growing food demands (Alexandratos and Bruinsma, 2012). However, deforestation and inappropriate agricultural practices have already degraded around 2 billion ha of the world's agricultural land (Pinstrup-Andersen and Pandya-Lorch, 1998). Satellite data show a decline in 12% of the global agricultural land from 1981 to 2003 (Nelleman *et al*., 2009). Moreover, escalating non-food crops demands raise concerns for having sufficient food crop production area (Popp *et al*., 2014; Searchinger and Heimlich, 2015). For example, in 2005, only 1% of biofuel was utilized for transport in the global fuel market; however, by 2050, biofuels are projected to increase up to 25% of the global fuel market (BCFN, 2010). In summary, population pressure, diminishing prime or good-quality land options (FAO, 2011), higher farm export market prices (Robertson and Swinton, 2005), and growing demand of non-food crop production area may create incentives to bring marginal land, currently unfit for agriculture, into production (Kendrick, 1983; Pimentel *et al.,* 2012; Gerwin *et al.,* 2018). Marginal land, including excessive steepness of grasslands,

hills, and uneven terrain (slope > 6˚), is unsafe for large conventional farm equipment. Tractor roll-overs are more frequent during farm operations on steep slopes and one of the leading causes of farmer injury or death (Myers *et al.,* 2009; Myers and Hendricks, 2010; Vigoroso *et al.,* 2019). Therefore, these steep grasslands are typically not suitable for agricultural vehicles (Foley *et al.,* 2011), and are usually used for grazing, particularly in the Great Plains, USA (Milchunas, 2006), which are characterized by gently rolling hills, steppe, and grasslands (USDA, 2020). The 2011 National Land Cover Database suggested that, within the 12 Great Plains states, an estimated 11.6 million ha of plains and grasslands are under shrubs or herbs, unprotected, and at a 6˚ to 25˚ slope (Homer *et al.,* 2015). There is a substantial potential to profitably increase food production on these steep grasslands and uneven terrains.

Therefore, a fleet of small autonomous ground vehicles (AGV) is envisioned to perform basic agricultural operations on steep slopes, hills, and uneven terrain. Multi-AGV is a fast-growing trend on smart farms (Blackmore et al*.,* 2002; Gonzalez-De-Santos *et al.,* 2020) and considered a prime candidate for future outdoor farms (Emmi *et al.,* 2014; Gonzalez-de Santos *et al.,* 2017; Gonzalez-De-Santos *et al.,* 2020). An AGV fleet accomplishes work equivalent to a large machine with reduced soil compaction, supports mission coordination and reconfiguration with improved safety (Pitla *et al*., 2010; Vougioukas, 2012; Emmi *et al*., 2013). The AGV can be programmed to perform almost all agricultural operations at peak efficiency, ranging from seeding to harvesting (Slaughter *et al*., 2008; Kondo *et al*., 2008; Bakker *et al*., 2010; Asimopoulos *et al*., 2013; Iida *et al*., 2017; Quaglia *et al*., 2019). However, it is imperative to understand how an individual AGV functions on sloping terrain under varying load and speed conditions, especially regarding traction, mobility, and power required. Moreover, the vehicle's boundary conditions must be established before planning a large-scale multi-AGV operation on sloped terrain.

Off-road vehicle performance varies with vehicle type, configuration, and intended function (Alcock, 1986; Wong, 2010; Creager *et al.,* 2017). The drawbar pull test has emerged as a valuable tool to

characterize off-road vehicle performance, e.g., tractors, cross-country, and space exploration vehicles (Creager *et al*., 2017). During a drawbar pull test, a vehicle must generate sufficient gross traction to counteract motion resistance and the applied drawbar pull. On soft soil or uphill run, an increase in drawbar pull force results in both increased wheel or track slip and energy losses. The vehicle can be immobilized, with sufficient drawbar pull which may restrict the multi-AGV operation on high slope terrain. The drawbar pull test measures the vehicle's total tractive ability, mobility, and energy consumption on specified soil conditions (Wong, 2010; Wettergreen *et al*., 2010). Three popular methods reported in the literature for drawbar pull testing of robots or ground vehicles are as follows: 1) testing a single traction element (track or wheel) in a soil bin (Ding *et al*., 2011; Gao *et al*., 2012; Sutoh *et al*., 2012; Senatore *et al*., 2013), 2) testing the entire vehicle in a soil bin (Al-Milli *et al*., 2010; Woodward, 2011; Wang *et al*., 2016) and 3) testing a vehicle in actual application environments (Park *et al.,* 2008; Ray *et al*., 2009). However, testing a single traction element typically does not represent the entire vehicle or system performance. Contrastingly, the actual application environment lacks test repeatability due to field variation which may introduce error. Moreover, operating a heavy ground vehicle on actual sloping terrain may be hazardous to both vehicle and operator during the testing. Hence, testing the entire AGV in a controlled soil bin environment seems appropriate.

In the last several decades, the drawbar pull performance of human-operated tractors, ground vehicles and robots has been extensively studied to optimize operational parameters and control variables, either on unprepared fields or in controlled soil bin environments (Esch *et al*., 1990; Molari *et al*., 2012; Keen *et al*., 2013; Kim *et al*., 2020). Soil conditions significantly influence the drawbar pull performance of off-road vehicles. Soil bin facilities have emerged as model laboratories for traction experiments for off-road vehicles (Ani *et al*., 2018). Soil bin facilities helped to evaluate the soil-machine interaction, traction element design and performance, and to optimize tractive efficiency for various off-road vehicles under

varying soil conditions. In most soil bin studies, the influence of soil properties (moisture content, bulk density, soil type, soil strength) on traction elements or vehicle performance has been extensively studied (Clark and Liljedahl, 1969; Wood and Burt, 1987; Way and Kishimoto, 2004; Sahu and Raheman, 2006; Ani *et al*., 2018). A soil bin capable of slopes from 0 to 11˚ was developed by Liu et al. (2002). Otherwise, no literature is available on varying the soil bin slope and its influence on vehicle performance.

In this study, a prime function of a prototype AGV is to traverse on level terrain and steep slopes (up to 20˚) with an adequate drawbar pull and load-carrying capacity to perform basic agricultural operations. Therefore, a drawbar pull test was performed on a prototype AGV to investigate the traction, mobility, and energy usage characteristics on level terrain and uphill and downhill travel on a variable slope ranging up to 20˚ at varying operating drawbar pull and speed. The drawbar pull performance test would quantify the AGV's available reserve power and help establish its performance curves (TOP 2-2-604, 2007). For a track vehicle, the test would measure the net traction developed by each track, while ascending and descending slopes, with or without additional applied drawbar pull. The magnitude of an additional drawbar pull would determine the nature of the agricultural operation (tillage type, seeding, spraying, harvesting, etc.) the AGV could perform on sloping terrain. This experimental investigation would be fundamental to understanding the limitations and capabilities of the AGV in a sloping environment. This study would also explore the suitability and establish the boundary conditions of small size ground vehicles for high slope farming. Another goal is to generate an AGV's traction database, which could be utilized to develop vehicle mobility models for highly sloped terrain. These models could predict specific dynamic responses, including power efficiency, travel reduction, energy consumption rate from inputs on a slope, applied drawbar pull, and vehicle speed. Mobility models could be used to optimize prototype design, components in path planning, and control algorithms that optimize multiple objectives including energy and time efficiency. The traction database is an important and first step towards developing the

AGV's mobility models.

## MATERIALS AND METHODS

### EXPERIMENTAL SETUP

#### *Autonomous Ground Vehicle (AGV)*

A continuous track-type AGV prototype, shown in figure 1, was used in this study. This skid-steer AGV was developed at the 2050 Robotics Laboratory (Kansas State University, Manhattan, KS, USA) to perform an agricultural operation on steep slopes and uneven terrain. The technical details of the AGV and traction element (tracks) are given in table 1. A positive drive sprocket drove each of the two rubber belts, which had teeth molded into their inner surfaces. The AGV is compact, so its overall width is less than a typical crop row spacing of 0.76 m, and is lightweight (102 kg). Additionally, it is equipped with an on-board microcontroller, a reconfigurable input-output device (myRIO, National Instruments, Austin, TX, USA) that requires a system-design platform in LabVIEW, proprioceptive sensors such as amperage (Analog 20 A Gravity series, dfrobot, Shanghai, China), voltage (30 VDC, Phidgets Inc., Calgary, Canada), and a track encoder (Encoder products, Sagle, Idaho, USA). The AGV was powered by a rechargeable 22.2 V, 13 Ah, and 15 C Lithium Polymer (Li-Po) battery (Venom Power, Rathdrum, Idaho, USA). The AGV accommodates the two battery packs and each battery pack includes two batteries connected in a parallel configuration which resulted in 26 Ah capacity. The prototype accommodates total two separate battery packs with a total amp-hour capacity of 52 Ah and 22.2 V, which is sufficient for at least 4-6 hours of continuous operation at standard operating conditions where AGV operates on concrete road without drawbar loading. The AGV was teleoperated and connected wirelessly via remote device software to a tablet computer (iPad, Apple Inc, Cupertino, CA).

**Table 1. Technical details of the AGV and fitted track**

| AGV | | Track | |
|---|---|---|---|
| Mass, kg | 102 | Track style | Continuous |
| Length, mm | 1160 | Thickness, mm | 5 |

| | | | |
|---|---|---|---|
| Width, mm | 640 | Belt width, mm | 50 |
| Height, mm | 550 | Belt contact length, mm | 2410 |
| Track gauge, mm | 500 | Diameter of sprockets (front) and idler (rear), mm | 126 |
| Longitudinal CG location from front roller axis, mm | 400 | Sprocket to idler center distance, mm | 910 |
| Longitudinal CG location from rear roller axis, mm | 700 | Lug height, mm | 12 |
| Vertical CG location, mm | 200 | Lug pitch, mm | 55 |
| Hitch height, mm | 200 | | |



**Figure 1. AGV used in the study.**

### Soil bin

An off-road vehicle's tractive ability is derived from the soil through its traction elements (Gill and Vanden Berg, 1967; Wong, 2010). The drawbar pull performance of a vehicle varies greatly with soil (Domier and Willans, 1978) and its conditions, i.e, soil moisture (Kim *et al*., 2019), bulk density and cone index (Hayes and Ligon, 1981). A soil bin (5.0 m long × 2.5 m wide × 0.2 m depth), fitted with a hydraulic lift attachment was used in the study. It provides an adjustable tilt bed (0˚-20˚) for vehicle testing in

horizontal straight runs and sloped runs, including uphill and downhill. The soil bin was filled with silt loam soil, and soil characteristics were evaluated in terms of soil bulk density on a dry basis (g/cm$^3$), water content (% dry basis), cone index (kPa) and cone index gradient (kPa/mm).

### *Instrumentation setup*

An instrumentation setup was established to measure the AGV's energy consumption, travel reduction, applied drawbar pull, and soil bin testbed characteristics. The AGV was equipped with amperage-voltage sensors and track encoders to measure its energy consumption and theoretical velocity, respectively. An S-type load cell (HT Sensor Technology Co., Ltd, Xi'an, China) with a capacity of 200 kg and ±0.02% accuracy was calibrated and used to measure the applied drawbar pull. The track encoder data were used to compute the velocity of the AGV track peripheries relative to the chassis i.e., theoretical velocity. A towed fifth wheel equipped with a shaft encoder (Encoder products, Sagle, Idaho, USA) was attached to the AGV chassis to measure vehicle travel velocity. However, the fifth wheel slipped on the testbed soil surface so, this initial fifth wheel was not successful and was replaced with a 3D-printed spool with a cotton thread wrapped around its circumference. During the experiments, the thread was tied to the soil bin frame. The thread wrapped and unwrapped along the spool circumference with respect to the AGV's position, and the encoder data were recorded. The spool-thread arrangement hereafter referred to as Ground Truth Encoder, measured the AGV travel velocity. The myRio microcontroller was accountable for AGV operation, data collection, and storage (via USB thumb-drive), and was connected to an iPad (tablet computer) via Wi-Fi.

The cone penetrometer test (CPT) is a test for *in situ* measurement of soil penetration resistance which is an indicator of soil firmness (Cohron *et al.,* 1971; ASAE Standards, 2018). A digital recording cone penetrometer (Rimik model: CP40II, Rimik Pvt. Ltd., Toowoomba, Australia) with a cone apex angle of 30˚ and base area of 323 mm$^2$ (ASABE Standards, 2019) was used to measure cone index (kPa) and cone index (CI) gradient (kPa/mm). In addition, a soil bulk density on a dry basis (d.b.) was measured with a

bulk density soil sampling kit (AMS Inc., American Falls, Idaho) using cylindrical soil cores 490 mm

diameter and 100 mm height. Gravimetric water content was determined using a standard oven-dry

method, with soil samples dried at 105˚C for 24 h. A digital protractor (Mini-MAG, Fowler High Precision,

Newton, MA, USA) was used to set the desired testbed slope.



**Figure 2. Drawbar pull test experimental setup: a) conceptual drawing, b) AGV operating on sloped soil bin. Direction of forward travel is from left to right.**

### Drawbar loading device

A rubber resistance band was used to apply drawbar pull to the AGV. The drawbar pull increased as the

stretching length of the rubber band increased and the magnitude of drawbar pull was not controlled with

any control system. One end of the resistance band was attached to the soil bin frame and the other to the

load cell, which was hooked to the AGV's hitch point, keeping the line of pull parallel to the soil bin

terrain (fig. 2). A load cell measured the applied drawbar pull. In this study, a ramped-drawbar pull test

technique (Woodward, 2011; Creager *et al.*, 2017) was implemented. Therefore, a complete range of

drawbar pull from zero (AGV self-propelled condition) to the maximum drawbar pull (100% slip) could

be observed in a single run. The experimental setup for conducting the drawbar pull test is shown in figure

2.

## EXPERIMENT DESIGN

### *Preparation of soil bin*

We strived to minimize variabilities in soil physical properties throughout the experiment. A soil

preparation method consisting of soil loosening, pulverization, and leveling was employed on each slope

as mentioned in (Creager *et al.,* 2017). However, repeated vehicle passes were compacting the soil,

cumulatively increasing the soil bulk density. A 15 tine bow rake (Model: 63141, Razor-Back professional

tools, Orlando, FL, USA) was used for soil preparation. This steel rake is perfect for loosening or breaking

up compacted soil and leveling the area. The trafficked soil was loosened and leveled with the rake.

The ramped- drawbar pull test was conducted on level terrain 0˚($S_0$) and sloping 10˚ and 18˚ terrain,

both uphill ($S_{10U}$ and $S_{18U}$) and downhill ($S_{10D}$ and $S_{18D}$). The range of AGV actual velocity was 1 to 5

m/min (table 2). During the experiment, the soil bin slope was first fixed and the AGV was operated at

each speed. Each experiment was replicated three times, and the independent variables and

response variables are shown in table 2. During each of the three replicates, the AGV was operated on

untrafficked soil. The soil bin is 2.5 m wide, and the single-track width is 50 mm, enabling multiple runs

of the AGV on untrafficked soil. The performance of the AGV was assessed in terms of metrics that relate

to traction analysis, vehicle mobility-immobility, and energy consumption.

**Table 2. Variables used in the experiment.**

| Predictor | | | Response |
|---|---|---|---|
| Slope (°) | Speed (m/min) | Drawbar pull (N) | |
| 0 ($S_0$) | 1.0 | | Power efficiency, η |
| 10 Uphill ($S_{10U}$) and Downhill ($S_{10D}$) | 2.0 | | Travel Reduction, s |
| 18 Uphill ($S_{18U}$) and Downhill ($S_{18D}$) | 3.0 | Variable Pull, 0-1500 | Power Number, PN |
| | 4.0 | | Energy consumption |
| | 5.0 | | Rate, ECR |

Vehicle traction ratio is the ratio of the drawbar pull ($P$) to the AGV's load normal to the tractive surface ($W$). The AGV's weight includes the vehicle weight and the weight of removable batteries. Traction ratio ($P/W$), allows a dissimilar vehicle weight comparison (Wong, 2010; Creager *et al.,* 2017). Travel reduction ($s$) indicates the reduction in the AGV's forward progress caused by shear within the soil, slip between the track and terrain, and flexing of the track (Wong, 2010; Creager *et al.,* 2017), and is defined as:

$$s = 1 - \frac{V}{V_t} \tag{1}$$

where $V$ is the AGV's actual velocity derived from the ground truth encoder. The theoretical velocity ($V_t$) is the product of track sprocket angular velocity and track rolling radius at the sprocket. The track angular velocity is derived from track encoder data. Power loss during the conversion process prevents the AGV from converting all electrical power into practical work. Therefore, a power efficiency, $\eta$, indicates the efficiency of an AGV in transferring the electrical power to an available drawbar power and is defined as:

$$\eta = \frac{P \times V}{P_B} \tag{2}$$

where $P_B$ is the power delivered by the battery and $P$ is the drawbar pull. We use "power efficiency" and not "tractive efficiency" because ASABE Standards (2013) defines tractive efficiency as the ratio of output power to input power for a traction device. The input power for the track is the axle power, which is the product of input torque applied to the track sprocket and the sprocket angular velocity. The input power which we measured is the electrical power delivered by the battery, which is not axle power and some power is lost because the efficiency of the motor and its circuitry in converting electrical power to motor output shaft power, is less than 100%.

The drawbar pull and vehicle velocity may influence the vehicle's power efficiency. The optimized power efficiency significantly improves the AGV's field performance (Lyne and Burt, 1989). There is an optimum range of drawbar pull or velocity that maximizes the PE. Hence, it is important to optimize

power efficiency by selecting the proper values of drawbar pull and velocity. A velocity loss or drawbar pull loss results in tractive inefficiency (Zoz and Grisso, 2003).

Battery capacity restricts the AGV's continuous operation, which would influence the mission planning and impact the overall efficiency of the multi-AGV system. Additionally, the AGV's speed, drawbar pull, and the slope may influence energy consumption. Therefore, it is important to establish the AGV's power-energy consumption characteristic curves on level and sloped terrain to optimize energy efficiency. Power Number (PN), defined as the ratio of power used to the product of the AGV's weight and velocity (eq. 3), quantifies mobility power cost. It estimates the power required to travel on a specific terrain with an external load, and is thus valuable for mission planning (Creager et al., 2017).

$$\text{PN} = \frac{P_B}{W \times V} \tag{3}$$

An energy consumption rate (ECR) is a distance-specific energy consumption expressed in Wh/km for electric vehicles derived from the PN. The ECR calculates the energy required (Wh) to travel one km distance (Freitag *et al.,* 1970; Freitag *et al.,* 1972) and is defined with equation 4. ECR measures the relative efficiency of the AGV while operating under different conditions, i.e., slope climbing or level terrain (Rooke, 2020).

$$\text{ECR} = \frac{\text{PN} \times \text{W}}{3.6} \tag{4}$$

**EXPERIMENTAL CONDITIONS**

***Drawbar pull test procedure***

Initially, the testbed slope was fixed, and the AGV was teleoperated at the desired speed (table 2). As the AGV moves on a testbed, the resistance band ramps up the *P* from zero to the maximum *P* until the AGV immobilizes i.e. 100% slip condition. This ramped- drawbar pull test technique permits a full *P* versus power efficiency (η) curve, *P* versus travel reduction, and *P* versus power number to be completed in a single run. Each experiment was replicated three times before proceeding to the next (table 2).

## Data collection and analysis

Before conducting the drawbar pull test, the testbed condition was measured, and the mean values were reported (table 3). The soil cone index (CI) was recorded for the 0-150 mm depth range at eight randomly selected locations on the testbed as per the ASAE standards (ASAE Standards, 2019). The CI gradient (kPa/mm) was computed from available data, which describes the soil's penetration resistance per unit depth (Creager *et al.,* 2017). Six soil cores for bulk density and water content were taken randomly on the testbed. During the drawbar pull test, data from the load cell, each track encoder, the ground-truth encoder, and the amperage-voltage sensors were recorded by a microcontroller (myRio) device at a frequency of 10 Hz. The response variables, power efficiency, and power number were calculated from the recorded sensor data (i.e., load cell and amperage-voltage sensors). The travel reduction was determined by comparing the theoretical velocity ($V_t$) to the actual velocity ($V$) (eq. 1). A multiple comparison procedure (Least significant difference, LSD) was used to analyze the testbed soil characteristics to ascertain if a significant difference existed among the soil properties CI, bulk density, and water content on the $S_0$, $S_{10}$ and $S_{18}$ terrain. The testbed slope with its $S_0$, $S_{10}$ and $S_{18}$ terrain conditions did not significantly affect CI, CI gradient, or water content. Testbed slope did significantly affect soil bulk density (P=0.02). A MATLAB program (Software version - R2018a, MathWorks, Natick, MA, USA) was used to generate a contour plot of dependent variables including power efficiency, travel reduction, and power number as a function of *P/W* and the AGV's speed.

**Table 3:   Testbed soil conditions and properties.**

| Testbed slope | Cone Index (kPa) [a] | CI gradient (kPa/mm) | Water content (% db) | Bulk density (g/cm$^3$) |
|---|---|---|---|---|
| 0 ($S_0$) | 493.3 ± 92.3[a] | 2.5 ± 0.5 [a] | 17.2 ± 4.0 [a] | 1.5± 0.1[a], [b] |
| 10 ($S_{10}$) | 464.4 ± 97.6 [a] | 2.4 ± 0.5 [a] | 18.8 ± 5.7 [a] | 1.4± 0.1 [a] |
| 18($S_{18}$) | 461.5 ± 59.8 [a] | 2.4 ± 0.3[a] | 18.5 ± 1.8 [a] | 1.6 ± 0.04 [b] |
| P-value | 0.59 | 0.73 | 0.77 | 0.02 |

[a] Within each column, mean values with the same letter are not significantly different at P=0.05 (LSD test).
Soil properties are recorded for the 0-150 mm depth range.

# RESULTS AND DISCUSSION

## TRACTION PERFORMANCE

The traction performance of the AGV on both level terrain ($S_0$) and sloping ($S_{10}$ and $S_{18}$) terrain was expressed in terms of power efficiency and travel reduction as a function of $P/W$ and the AGV's speed, are shown in figures 3 and 4, respectively. A general shape of the PE performance curve shows that PE increased as $P/W$ increased, reaching the peak and maintaining it for a small range of $P/W$, as illustrated in figure 3. After reaching the peak, PE starts to decline with further increase in $P/W$ while the travel reduction rapidly increases after hitting the maximum $P/W$ value, eventually immobilizing the AGV when track slip reached 100% (fig. 4). The PE contour plot depicts an efficient zone of operation, indicating that the maximum desirable driving condition is at the $P/W$ and speed setting, where travel reduction is at a minimum and PE is at the peak. The efficient zone of the AGV operation, on a level terrain ($S_0$), was observed at $\geq 3$ m/min speed and 0.50-0.60 $P/W$ range, where PE was 0.20, and travel reduction was 0.10 (fig. 3 and table 4).

**Table 4: Tractive performance of AGV on sloped terrain.**

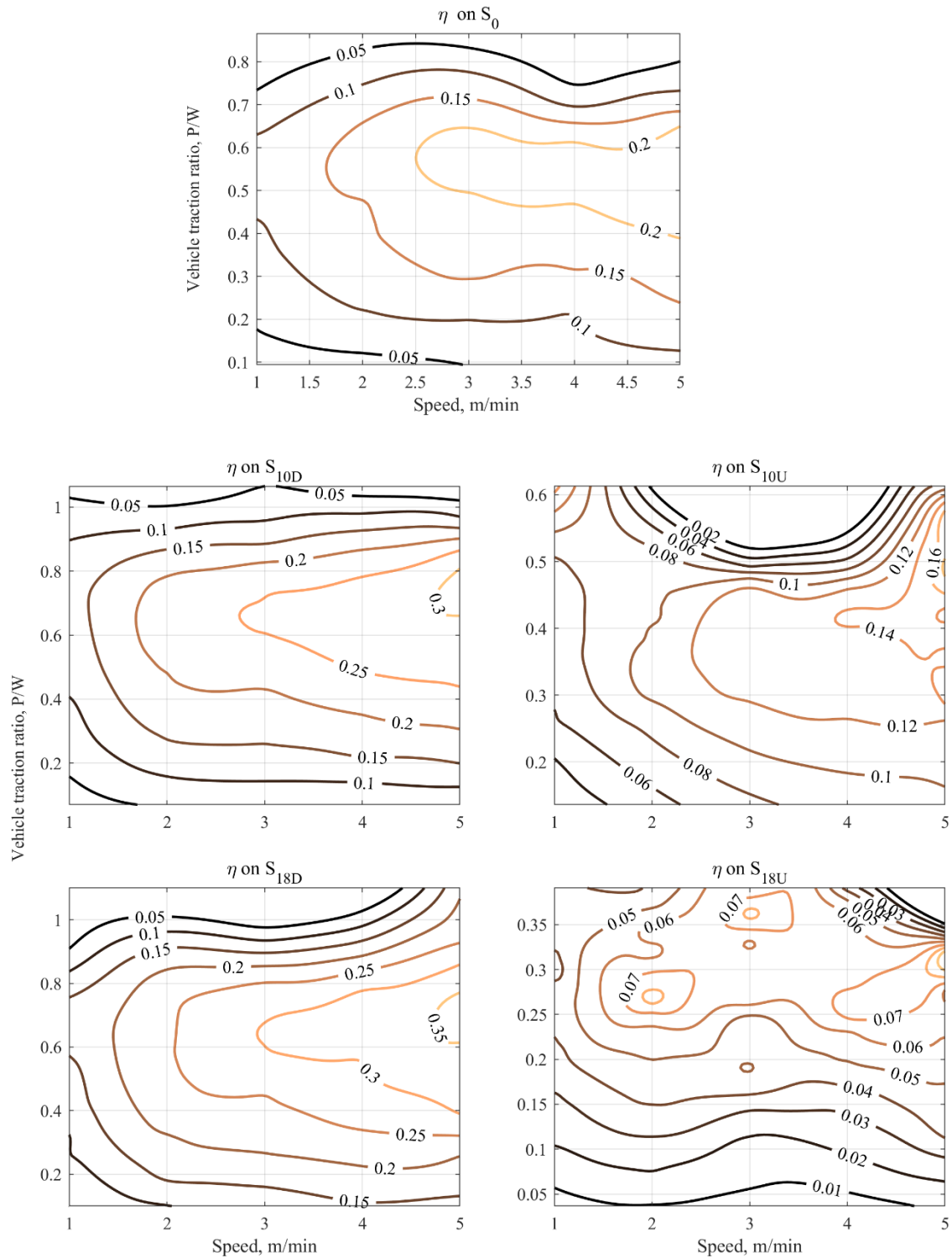|  | Slope condition | | | | |
|---|---|---|---|---|---|
|  | $S_0$ | $S_{10D}$ | $S_{18D}$ | $S_{10U}$ | $S_{18U}$ |
| $\eta_{max}$ | 0.20 | 0.25 | 0.30 | 0.12 | 0.07 |
| $P/W$ at $\eta_{max}$ | 0.55 | 0.70 | 0.70 | 0.45 | 0.30 |
| $TR$ at $\eta_{max}$ | 0.10 | 0.10 | 0.10 | 0.20-0.30 | 0.20-0.30 |
| $PN$ at $\eta_{max}$ | 2-3 | 3 | 3 | 4-7 | 4-7 |
| Efficient zone | 0.50-0.60 $P/W$ | 0.50-0.70 $P/W$ | 0.50-0.70 $P/W$ | 0.35-0.55 $P/W$ | 0.25-0.35 $P/W$ |

**Figure 3. Power efficiency, *η*, as a function of vehicle speed and traction ratio, *P/W*, for AGV traveling on level surface, downhill slope, and uphill slope.**

The AGV is capable of generating drawbar pull equal to its weight, traction ratio of 1, at the cost of

reduced PE which was observed only on the downhill operation $\eta \leqslant 0.5$ and $\eta \approx 0.10$ on $S_{10D}$, and $S_{18D}$, respectively (fig. 3). However, the peak PE observed on $S_0$, $S_{10D}$, and $S_{18D}$ was 0.20, 0.25 and 0.30 at 0.55, 0.70, and 0.70 *P/W*, respectively, illustrating that the maximum PE and the maximum *P/W* cannot be achieved simultaneously (Garber, 1985). On the other hand, the AGV is unable to generate a drawbar pull equivalent to its weight on the level surface and uphill operation. The maximum *P/W* was 0.80 for $S_0$, 0.60 for $S_{10U}$, and 0.35 for $S_{18U}$ (fig. 3).
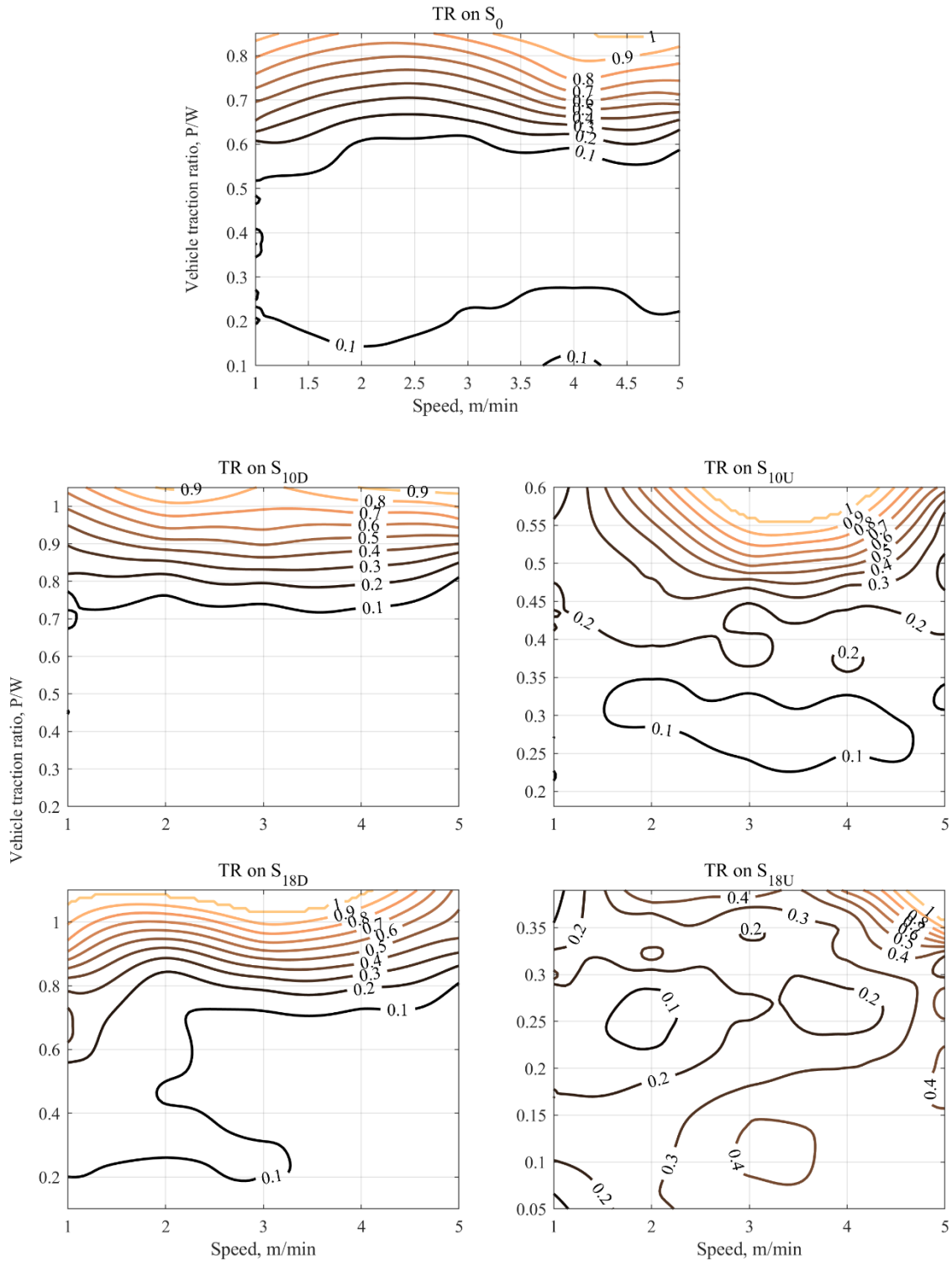
**Figure 4. Travel reduction, *s* (decimal), as a function of vehicle speed and traction ratio, *P/W*, for AGV travelling on level surface, downhill slope, and uphill slope.**

On a level terrain (S₀), the AGV's peak PE was 0.20, observed at 0.50-0.60 *P/W* range and ≥3 m/min

speed with a travel reduction of around 0.10. However, AGV's downhill operation (10 to 18°) shows a significant increase in peak PE with a slight increase in $P/W$. The peak PE increased by 25% and 50% on slopes 10° ($S_{10D}$) and 18°($S_{18D}$), respectively, compared to 0°($S_0$) with a slight increase in $P/W$ from 0.55 to 0.70 (fig. 3). The maximum recorded PE was 0.30, observed on 18°($S_{18D}$) at a 0.50-0.70 $P/W$ range and $\geq$ 3 m/min speed with travel reduction ranging between 0.10 and 0.20. However, the AGV's uphill slope (0-18°) operation shows a significant PE decline. The peak PE decreases from 0.20 to 0.12 to 0.7, on 0°($S_0$), 10°($S_{10U}$), and 18°($S_{18U}$), respectively, with a subsequent decline in $P/W$ from 0.55 to 0.45 to 0.30 $P/W$, respectively (fig. 3). Peak PE decreased by 30% and 65% on slope 10°($S_{10U}$) and 18°($S_{18U}$), respectively, compared to 0°($S_0$). This decrease in peak PE could be explained by an increase in the travel reduction from 0.10 to 0.30 on 0°($S_0$) and on both 10 and 18° ($S_{10U}$ and $S_{18U}$), respectively (table 4 and fig. 4). Operating the AGV at speed $\leq$ 2m/min was less efficient for the PE than speed $\geq$ 3m/min, except on $S_{18U}$.

The AGV on 10° slope results in the peak PE of 0.25 at 0.70 $P/W$ and 0.12 at 0.45 $P/W$ on $S_{10D}$ and $S_{10U}$, respectively (fig. 3). This AGV's downhill operation generates 108.3% higher PE than the uphill operation with a 55.5% increase in $P/W$. Similarly, on the 18° slope, peak PE was 0.30 at 0.70 $P/W$ and 0.07 at 0.30 $P/W$ on $S_{18D}$ and $S_{18U}$, respectively (fig. 3). This AGV's downhill operation generates 328.6% higher PE than the uphill operation with a 133% increase in $P/W$. The uphill operation shows a significantly lower PE and $P/W$ than a downhill operation, which could be explained by the increase in travel reduction from 0.10 to 0.30 (fig. 4). In other words, there was a 200% increase in travel reduction for both 10° and 18° compared to 0° slope (table 4). The fact that AGV operation is more efficient on a downhill than an uphill slope may sound trivial, but these generated data will be a prerequisite to develop or train mobility models on a sloping terrain environment.

The phenomenon of increase in PE with downhill slope, and decreases in PE with uphill slope is

explained by the AGV's free body diagram on an inclined plane (fig. 5). The gravity force ($f_g$) on an incline is resolved into two force components: parallel ($f_{//}$) and perpendicular ($f_\perp$). On a level terrain ($\theta = 0$), $f_{//}$ becomes zero and $f_\perp$ is at the maximum, balancing the normal force ($f_n$) and gravity force ($f_g$). As slope angle ($\theta$) increases from 0° to 18°, the magnitude of $f_{//}$ increases, and $f_\perp$ decreases. Thus, $f_\perp$ directed opposite to $f_n$, keeping the balance. However, the unbalanced $f_{//}$ increases the net force acting on the AGV. The presence of unbalanced $f_{//}$ (gravity force component) increases with slope angle ($\theta$). The $f_{//}$ causes the AGV to accelerate down the incline. There was greater gravity-induced acceleration of the AGV with a greater slope angle, resulting in higher PE for $S_{18D}$ compared to $S_{10D}$. The presence of motion resistance would oppose the AGV gravity-induced acceleration. However, this resulting acceleration becomes negative in the case of an uphill operation, pulling the AGV downslope, subsequently increasing the travel reduction and reducing the PE for both $S_{10U}$ and $S_{18U}$ (fig. 3 and fig. 4). The AGV's weight transfer and its effect on the track-soil contact pressure distribution may also help explain the AGV's behavior on sloping terrain, but this is not within the scope of the study.
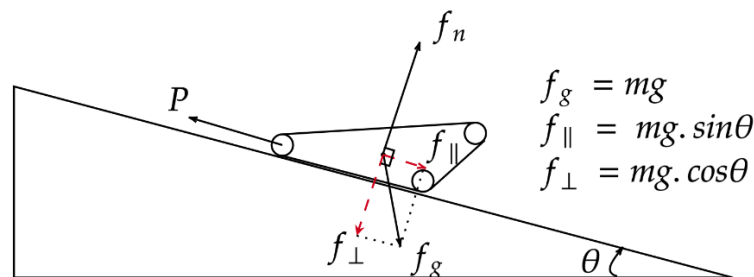


**Figure 5. Free body diagram explaining the forces acting on AGV, on a slope.**

Any drawbar pull exerted to the AGV's hitch point will produce the AGV's travel reduction, due to a track-soil slip and losses within traction elements. Figure 4 indicates the range of *P/W* that delivers the optimum travel reduction (0.10-0.20) and maximum achievable *P/W*, the AGV can operate before becoming immobilized (s = 100%). The AGV maintains the optimum travel reduction ⩽0.20 for a wide

range of *P/W* before reaching the limiting *P/W* (i.e., maximum value of *P/W)* that rapidly increases the travel reduction. The limiting *P/W* was observed to vary with the slope angle and was 0.60, 0.80, and 0.80 on $S_0$, $S_{10D}$ and $S_{18D}$, respectively (fig. 5). On $S_0$, TR less than 10% was observed for a traction ratio of 0.55-0.60, and after that, TR increases monotonically as the vehicle traction ratio increases (figure 4). A similar trend was observed in Zoz and Grisso (2003) for large agricultural tractors, where TR of less than 10% was observed for a traction ratio of 0.50, and after that, TR increases as the vehicle traction ratio increases. These small AGV' traction performance was in good agreement with big agricultural tractors traction performance results reported in Zoz and Grisso (2003). However, on the uphill slope, a gravity-induced acceleration ($f_{//}$) applies a downslope pulling force to the AGV, increasing travel reduction from 0.10 to 0.30, respectively, on $S_0$ and both $S_{10U}$ and $S_{18U}$. Crossing the limiting *P/W* on an uphill slope does not immobilize the AGV, but pulls the AGV in the direction of the drawbar pull vector. This uncontrolled rapid slide may result in a collision either with an adjacent operating AGV in multi-AGV systems. The AGV was unable to generate substantial PE with applied drawbar pull on $S_{18U}$, which may restrict the nature of the agricultural operation the AGV could perform on uphill slope greater than 18˚.

**MOBILITY ENERGY CONSUMPTION**

An AGV operating on sloping terrain at a minimum energy consumption is desirable. The mobility energy consumption of the AGV on level terrain ($S_0$) and sloping ($S_{10}$ and $S_{18}$) terrain was expressed in terms of power number, as a function of *P/W* and the AGV's speed, as shown in figure 6. The higher the power number the higher the energy consumption. The general shape of power number curves indicates that an increase in *P/W* increases the power number (fig. 6). The *P/W* influence the travel reduction and PN, which further influence the AGV mobility cost. The PN is less than 4 as long as the AGV's travel reduction is around 10% and it increases to a higher value before approaching infinity as travel reduction increases to 100%. The contour plots in Fig. 6 depict a maximum PN of 20. A PN values of infinity

corresponds to 100% travel reduction because the vehicle would be expending all its energy as its tracks would be spinning in its place, thereby increasing the cost of mobility.

The contour plots reveal the boundary conditions of PN corresponding to $P$ on a slope taken under the study. The downhill operation shows a slightly lower PN than the uphill operation, with an increased $P/W$. The PN corresponding to the peak PE is summarized in table 4. The developed PN versus $P/W$ chart for each slope can be used to estimate the power required to travel on a specific terrain with drawbar load. Hence, this is very useful for mission planning of multi-AGV systems on various terrains.

The ECR computes the AGV's energy expenditure and battery replacement frequency from the available power number data. The ECR at peak PE was calculated with the corresponding power number, and it was 1.0 kWh/km (PN= 3) on $S_0$, $S_{10D}$ and $S_{18D}$, and 2.0 kWh/km (PN= 6) on $S_{10U}$ and $S_{18U}$.
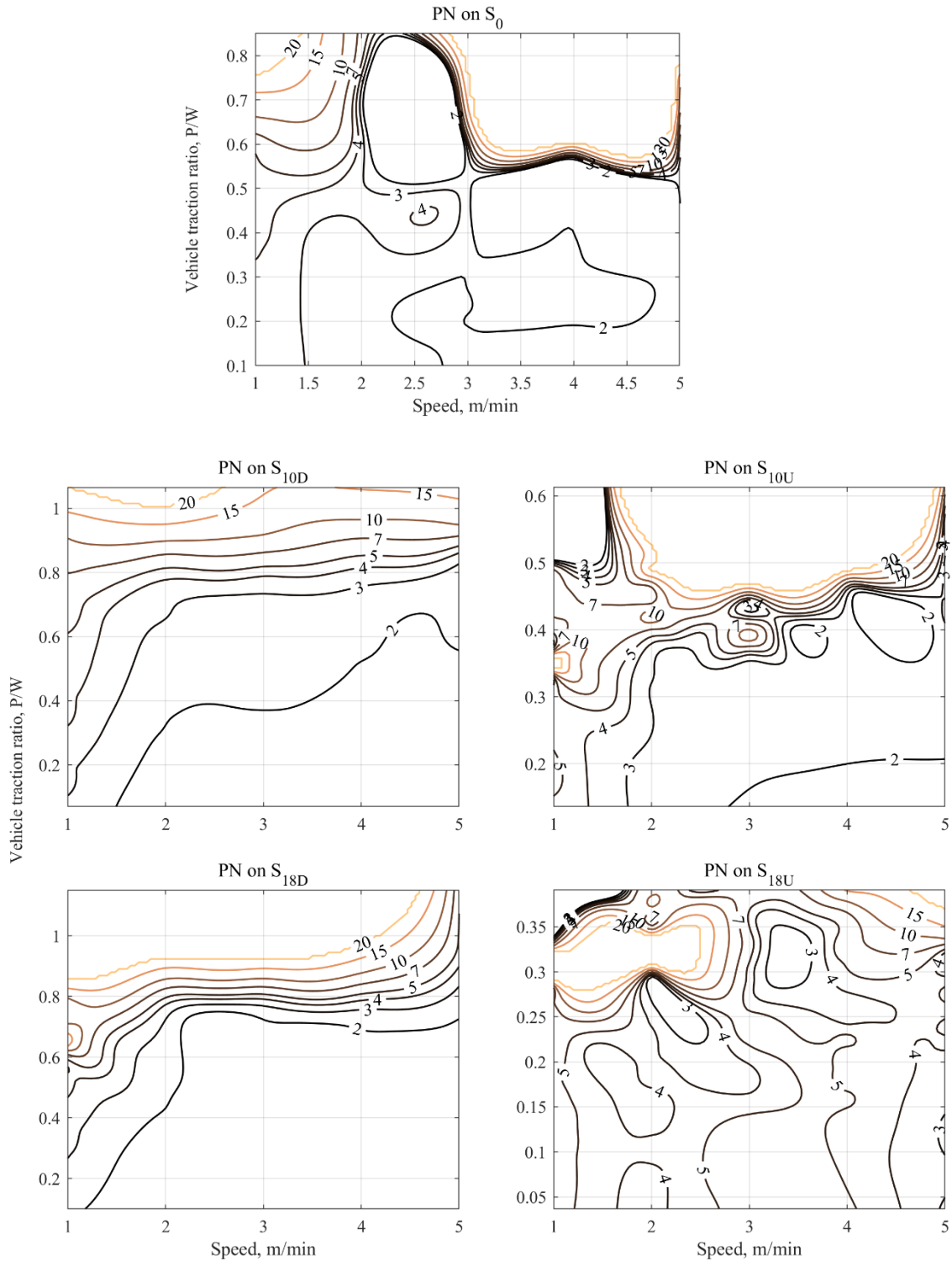
**Figure 6. Power number, *PN*, as a function of vehicle speed and traction ratio, *P/W*, for AGV travelling on level surface, downhill slope, and uphill slope.**

The study also aimed to generate an AGV's traction-mobility database and characteristic curves on level terrain and variable slopes from -20° to 20° at varying operating drawbar pull and speeds. During the experiment, an efficient zone of AGV operation (maximum PE for a given set of *P/W* and speed) was found to shift with the slope angle and direction of travel (uphill and downhill). To maximize the AGV's performance, it is important to monitor the shifting efficient zone for each slope angle and direction. Applying *P/W* beyond the limiting value immobilized the AGV, resulting in 100% travel reduction. However, the optimum range of *P/W* gives the minimum travel reduction and would decide the nature of the agricultural operation the AGV could perform on a slope. Moreover, peak PE and peak *P/W* cannot be achieved simultaneously; thus, it is necessary to prioritize between peak PE or peak *P/W*, depending upon the agricultural operation. The AGV was unable to generate significant PE with applied drawbar pull on an uphill slope (18°), eventually causing the AGV to slide in the direction of the drawbar pull vector, which could jeopardize the operation of the entire multi-AGV system. The AGV's operational variables, such as speed and *P/W* need to be optimized to maximize the AGV's performance on sloping terrain. To make all these decisions in a dynamic environment, there needs to be a centralized routing algorithm. The data on PE and travel reduction could be utilized to develop a central decision-making algorithm, which generates vehicle mobility, design, safety, and route-optimization models for highly sloped soil terrain. The power number data would be used for mission planning, energy optimization, battery swapping frequency, and path optimization models since, for a given *P/W,* the cost of going uphill is greater than the cost of going downhill. This would assist in achieving an efficiently powered multi-AGV system. Also, before the AGV's actual field operation, computer simulations can be performed on a digital terrain model for the desired slope to check and predict the AGV's application feasibility and go-no-go situation. The developed centralized algorithm or models generated from a traction database in a controlled laboratory environment can be extended to a sloping environment. These models would predict specific dynamic responses,

including PE, travel reduction, and power numbers from inputs including duty cycle, *P/W*, terrain slope, and soil characteristics (fig. 7).
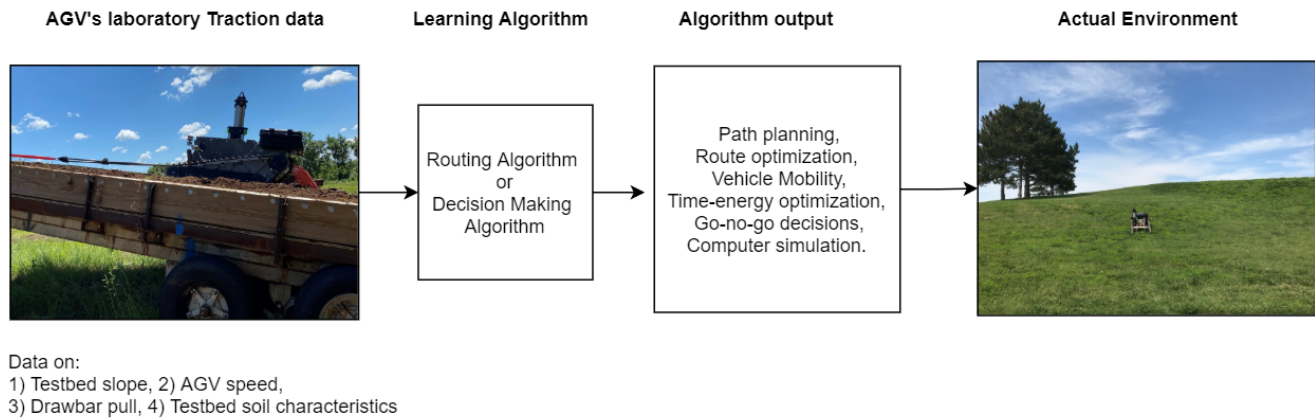


**Figure 7. Traction data application for proposed multi-AGV system.**

## Conclusions

A prototype AGV's tractive performance was evaluated on a level terrain and variable slope up to 18° (both uphill and downhill) at varying drawbar pull and operating speed conditions on a soil bin. The performance was expressed in power efficiency, travel reduction, power number and energy consumption rate. From the observed data, the following conclusions can be drawn.

- The AGV generates a drawbar pull equivalent to own weight (*P/W* = 1) at the cost of reduced PE only on downhill slope. Maximum PE and maximum *P/W* cannot be achieved simultaneously. However, the AGV on the uphill slope resulted in significantly lower *P/W* and the maximum value of 0.6 and 0.4 *P/W* was observed on 10° and 18° uphill, respectively.

- Power efficiency increases with an increase in the downhill slope angle with a slight increase in *P/W* and is significantly higher for downhill than uphill operations for the same slope angle but with a significant increase in drawbar pull. Power efficiency increased by 25% and 50% on 10° and 18° downhill slopes, respectively compared to 0°. Power efficiency was 108.3% and 328.6%

higher on the downhill than uphill run with a 55.5% and a 133% increase in *P/W*, on 10˚ and 18˚ slopes, respectively.

- Travel reduction is a major source of power loss caused by applying drawbar pull. However, the AGV maintains the optimum TR ≤ 20% for a wide range of *P/W* before reaching the limiting *P/W* 0.60, 0.80, and 0.80 on 0˚, 10˚ and 18˚ downhill slopes, respectively.

- The optimum values of power number ranged from 2 to 4. The ECR, at maximum PE, ranged from 1.0 kWh/km to 2.0 kWh/km.

In summary, the AGV delivered optimum power efficiency and generated enough drawbar pull with optimum travel reduction and power number. This study found that the prototype AGV can successfully operate on slopes up to 18˚, so with high sloped terrain or hills could be farmed with the proposed multi-AGV system. Nevertheless, a multi-AGV system serving on high sloped terrain needs a robust and efficient decision-making algorithm to predict and optimize the AGV's operating parameters on various terrains.

**REFERENCES**

Al-Milli, S., Seneviratne, L. D., and Althoefer, K. (2010). Track–terrain modelling and traversability prediction for tracked vehicles on soft terrain. *Journal of Terramechanics*, 47(3):151–160.

Alcock, R. (1986). Vehicle Performance. In Tractor-Implement Systems, pp. 92–108. Springer US, Boston, MA.

Alexandratos, N. and Bruinsma, J. (2012). World agriculture: towards 2030/2050 – the 2012 revision. ESA Working paper 12-03., FAO, Rome.

Ani, O. A., Uzoejinwa, B., Ezeama, A., Onwualu, A., Ugwu, S., and Ohagwu, C. (2018). Overview of soil-machine interaction studies in soil bins. *Soil and Tillage Research*, 175:13–27.

ASAE Standards. (2013). S296.5: General terminology for traction of agricultural traction and transport devices and vehicles. St. Joseph, MI: ASABE.

ASAE Standards (2018). S313.3:Soil Cone Penetrometer. St. Joseph, MI: ASABE.

ASAE Standards (2019). EP542.1: Procedures for Using and Reporting Data Obtained with the Soil Cone Penetrometer. St. Joseph, MI: ASABE.

Asimopoulos, N., Parisses, C., Smyrnaios, A., and Germanidis, N. (2013). Autonomous Vehicle for Saffron Harvesting. *Procedia Technology*, 8:175–182.

Bakker, T., Asselt, K., Bontsema, J., Muller, J., and Straten, G. (2010). Systematic design of an autonomous platform for robotic weeding. *Journal of Terramechanics*, 47(2):63–73.

BCFN (2010). The challenges of food security. Technical report, Barilla Center For Food and Nutrition.

Blackmore, S., Have, H., and Fountas, S. (2002). Specification of Behavioural Requirements for an Autonomous Tractor. In *Automation Technology for Off-Road Equipment Proceedings of the 2002 Conference*. ASABE.

Clark, S. J. and Liljedahl, J. B. (1969). Model Studies of Single, Dual and Tandem Wheels. *Transactions of the ASAE*, 12(2):0240–0245.

Cohron, G. T., Costes, N. C., and Moss, D. C. (1971). Cone penetration resistance test- An approach to evaluating in-place strength and packing characteristics of lunar soils. *Proceedings of the Lunar Science Conference*, 2:1973.

Costanza, R., Cumberland, J. H., Daly, H. E., Goodland, R. J. A., Norgaard, R. B., Kubiszewski, I., and Franco, C. (2015). *An introduction to ecological economics* ( 2nd ed). CRC Press Boca Raton, FL.

Creager, C., Asnani, V., Oravec, H., and Woodward, A. (2017). Drawbar Pull (DP) Procedures for Off-Road Vehicle Testing. Technical Report NASA/TP-2017-219384, E-19292, GRC-E-DAA-TN31725, NASA.

Ding, L., Gao, H., Deng, Z., Nagatani, K., and Yoshida, K. (2011). Experimental study and analysis on driving wheels' performance for planetary exploration rovers moving in deformable soil. *Journal of Terramechanics*, 48(1):27–45.

Domier, K. and Willans, A. (1978). Tractive efficiency–maximum or optimum? *Transactions of the ASAE*,

21(4):650–0653.

Emmi, L., Gonzalez-de Soto, M., Pajares, G., and Gonzalez-de Santos, P. (2014). New Trends in Robotics for Agriculture: Integration and Assessment of a Real Fleet of Robots. *The Scientific World Journal*, 2014:1–21.

Emmi, L., Paredes-Madrid, L., Ribeiro, A., Pajares, G., and Gonzalez-de-Santos, P. (2013). Fleets of robots for precision agriculture: a simulation environment. *Industrial Robot: An International Journal*, 40(1):41–58.

Esch, J. H., Bashford, L. L., Von Bargen, K., and Ekstrom, R. E. (1990). Tractive Performance Comparison Between a Rubber Belt Track and a Four-Wheel-Drive Tractor. *Transactions of the ASAE*, 33(4):1109– 1115.

FAO (2011). FAO in the 21st century ensuring food security in a changing world. Technical report, FAO, Rome.

Foley, J. A., Ramankutty, N., Brauman, K. A., Cassidy, E. S., Gerber, J. S., Johnston, M., Mueller, N. D., O'Connell, C., Ray, D. K., West, P. C., Balzer, C., Bennett, E. M., Carpenter, S. R., Hill, J., Monfreda, C., Polasky, S., Rockström, J., Sheehan, J., Siebert, S., Tilman, D., and Zaks, D. P. M. (2011). Solutions for a cultivated planet. *Nature*, 478(7369):337–342.

Freitag, D., Green, A., and Melzer, K. (1970). Performance evaluation of wheels for lunar vehicles (Summary report). Technical Report M-70-4, NASA.

Freitag, D., Green, A., Melzer, K.-J., and Costes, N. (1972). Wheels for lunar vehicles. *Journal of Terramechanics*, 8(3):89–105.

Gao, H., Li, W., Ding, L., Deng, Z., and Liu, Z. (2012). A method for on-line soil parameters modification to planetary rover simulation. *Journal of Terramechanics*, 49(6):325–339.

Garber, M. (1985). Tractive efficiency of a tracked vehicle. *Journal of Agricultural Engineering Research*, 32(4):359–368.

Gerwin, W., Repmann, F., Galatsidas, S., Vlachaki, D., Gounaris, N., Baumgarten, W., Volkmann, C., Keramitzis, D., Kiourtsis, F., and Freese, D. (2018). Assessment and quantification of marginal lands for biomass production in europe using soil-quality indicators. *Soil*, 4(4):267–290.

Gill, W. R. and Vanden Berg, G. E. (1967). Soil dynamics in tillage and traction. Washington, D.C.: Agricultural Research Service, USDA.

Gonzalez-De-Santos, P., Fern´andez, R., Sepu´lveda, D., Navas, E., and Armada, M. (2020). Unmanned Ground

Vehicles for Smart Farms. In *Agronomy [Working Title]*. IntechOpen.

Gonzalez-de Santos, P., Ribeiro, A., Fernandez-Quintanilla, C., Lopez-Granados, F., Brandstoetter, M., Tomic, S., Pedrazzi, S., Peruzzi, A., Pajares, G., Kaplanis, G., Perez-Ruiz, M., Valero, C., del Cerro, J., Vieri, M., Rabatel, G., and Debilde, B. (2017). Fleets of robots for environmentally-safe pest control in agriculture. *Precision Agriculture*, 18(4):574–614.

Hayes, J. C. and Ligon, J. T. (1981). Traction Prediction Using Soil Physical Properties. *Transactions of the ASAE*, 24(6):1420–1425.

Homer, C., Dewitz, J., Yang, L., Jin, S., Danielson, P., Xian, G., Coulston, J., Herold, N., Wickham, J., and Megown, K. (2015). Completion of the 2011 National Land Cover Database for the Conterminous United States-Representing a Decade of Land Cover Change Information. *Photogrammetric Engineering and Remote Sensing*, 81(5):346–354.

Iida, M., Harada, S., Sasaki, R., Zhang, Y., Asada, R., Suguri, M., and Masuda, R. (2017). Multi-Combine Robot System for Rice Harvesting Operation. In *2017 Spokane, Washington:* ASABE.

Keen, A., Hall, N., Soni, P., Gholkar, M. D., Cooper, S., and Ferdous, J. (2013). A review of the tractive performance of wheeled tractors and soil management in lowland intensive rice production. *Journal of Terramechanics*, 50(1):45–62.

Kendrick, J. (1983). *Water-related Technologies for Sustainable Agriculture in U.S. Arid/semiarid Lands*. Congress of the United States, Office of Technology Assessment. Google-Books-ID: i8iwX5xIWqQC.

Kim, W. S., Kim, Y. J., Baek, S. Y., Baek, S. M., Kim, Y. S., Choi, Y., Kim, Y. K., and Choi, I. S. (2020). Traction performance evaluation of a 78-kW-class agricultural tractor using cone index map in a Korean paddy field. *Journal of Terramechanics*, 91:285–296.

Kim, W. S., Kim, Y. J., Park, S. U., Nam, K. C., and Choi, C. H. (2019). Analysis of traction performance for an agricultural tractor according to soil moisture content during plow tillage. In *2019 Boston, Massachusetts:* ASABE.

Kondo, N., Yamamoto, K., Yata, K., and Kurita, M. (2008). A Machine Vision for Tomato Cluster Harvesting Robot. In *2008 Providence, Rhode Island:* ASABE.

Liu, J., Lobb, D. A., & Chen, Y. (2002). Innovative design features of a soil bin to facilitate research on soil tool interaction. ASABE Paper No. 021136. St. Joseph, MI: ASABE.

Lyne, P. W. L. and Burt, E. C. (1989). Real-Time Optimization of Tractive Efficiency. *Transactions of the ASAE*, 32(2):0431–0435.

Milchunas, D. G. (2006). Responses of plant communities to grazing in the southwestern United States. Gen. Tech. Rep. RMRS-GTR-169. Fort Collins, CO: USDA, Rocky Mountain Research Station. 126 pp. 169.

Molari, G., Bellentani, L., Guarnieri, A., Walker, M., and Sedoni, E. (2012). Performance of an agricultural tractor fitted with rubber tracks. *Biosystems Engineering*, 111(1):57 – 63.

Myers, J. R. and Hendricks, K. J. (2010). Agricultural tractor overturn deaths: Assessment of trends and risk factors. *American Journal of Industrial Medicine*, 53(7):662–672.

Myers, M. L., Cole, H. P., and Westneat, S. C. (2009). Injury severity related to overturn characteristics of tractors. *Journal of Safety Research*, 40(2):165–170.

Nelleman, C., Macdevette, M., Manders, T., Eickhout, B., Svihus, B., and Gerdien Prins, A. (2009). The Environmental Food Crisis: the environment's role in averting future food crises. Technical 978-827701-054-0, United Nations.

Park, W., Chang, Y., Lee, S., Hong, J., Park, J., and Lee, K. (2008). Prediction of the tractive performance of a flexible tracked vehicle. *Journal of Terramechanics*, 45(1-2):13–23.

Pimentel, D., Cerasale, D., Stanley, R., Perlman, R., Newman, E., Brent, L., Mullan, A., and Chang, D. (2012). Annual vs. perennial grain production. *Agriculture, Ecosystems and Environment*, 161:1–9.

Pinstrup-Andersen, P. and Pandya-Lorch, R. (1998). Food security and sustainable use of natural resources: a 2020 vision. *Ecological Economics*, 26(1):1 – 10.

Pitla, S. K., Luck, J. D., and Shearer, S. A. (2010). Multi-Robot System Control Architecture (MRSCA) for Agricultural Production. In *2010 Pittsburgh, Pennsylvania:*ASABE.

Popp, J., Lakner, Z., Harangi-R´akos, M., and F´ari, M. (2014). The effect of bioenergy expansion: Food, energy, and environment. *Renewable and Sustainable Energy Reviews*, 32:559-578.

Quaglia, G., Visconte, C., Scimmi, L. S., Melchiorre, M., Cavallone, P., and Pastorelli, S. (2019). Design of the

positioning mechanism of an unmanned ground vehicle for precision agriculture. In *Advances in Mechanism and Machine Science*, Mechanisms and Machine Science, pp 3531–3540, Cham. Springer International Publishing.

Ray, L. R., Brande, D. C., and Lever, J. H. (2009). Estimation of net traction for differential-steered wheeled robots. *Journal of Terramechanics*, 46(3):75–87.

Robertson, G. P. and Swinton, S. M. (2005). Reconciling agricultural productivity and environmental integrity: a grand challenge for agriculture. *Frontiers in Ecology and the Environment*, 1(3):38–46.

Rooke, K. (2020). Tesla Vehicle Efficiency: The Gold Standard Among EVs.

Sahu, R. and Raheman, H. (2006). Draught Prediction of Agricultural Implements using Reference Tillage Tools in Sandy Clay Loam Soil. *Biosystems Engineering*, 94(2):275–284.

Searchinger, T. and Heimlich, R. (2015). Avoiding Bioenergy Competition for Food Crops and Land. Technical report, Working Paper, Installment 9 of Creating a Sustainable Food Future. Washington, DC: World Resources Institute.

Senatore, C., Jayakumar, P., and Iagnemma, K. (2013). Experimental Study of Lightweight Tracked Vehicle Performance on Dry Granular Materials. Technical report, Army Tank Automotive Research Development and Engineering Center. Warren, MI.

Slaughter, D., Giles, D., and Downey, D. (2008). Autonomous robotic weed control systems: A review. *Computers and Electronics in Agriculture*, 61(1):63–78.

Sutoh, M., Yusa, J., Ito, T., Nagatani, K., and Yoshida, K. (2012). Traveling performance evaluation of planetary rovers on loose soil. *Journal of Field Robotics*, 29(4):648–662.

TOP 2-2-604 (2007). Test Operations Procedure (TOP) 2-2-604 Drawbar Pull. Technical Report :0704-0188, Combat and Automotive Systems Division, US Army Yuma Test Center, Yuma, AZ 85365.

USDA (2020). The Great Plains including the Black Hills - Grassland, Shrubland and Desert Ecosystems - RMRS. publisher: USDA- Forest Service and Rocky Mountain Research Station.

Vigoroso, L., Caffaro, F., and Cavallo, E. (2019). Warning against Critical Slopes in Agriculture: Comprehension of Targeted Safety Signs in a Group of Machinery Operators in Italy. *International Journal of Environmental Research and Public Health*, 16(4).

Vougioukas, S. G. (2012). A distributed control framework for motion coordination of teams of autonomous agricultural vehicles. *Biosystems Engineering*, 113(3):284–297.

Wang, M., Wu, C., Ge, T., Gu, Z. M., and Sun, Y. H. (2016). Modeling, calibration and validation of tractive performance for seafloor tracked trencher. *Journal of Terramechanics*, 66:13–25.

Way, T. R. and Kishimoto, T. (2004). Interface Pressures of a Tractor Drive Tyre on Structured and Loose Soils. *Biosystems Engineering*, 87(3):375–386.

Wettergreen, D., Moreland, S., Skonieczny, K., Jonak, D., Kohanbash, D., and Teza, J. (2010). Design and field experimentation of a prototype Lunar prospector. *The International Journal of Robotics Research*, 29(12):1550–1564.

Wong, J. (2010). Performance of off-road vehicles. In *Terramechanics and Off-Road Vehicle Engineering (Second Edition)*, pages 129 – 153. Butterworth-Heinemann, Oxford.

Wood, R. K. and Burt, E. C. (1987). Thrust and Motion Resistance from Soil-Tire Interface Stress Measurements. *Transactions of the ASAE*, 30(5):1288–1292.

Woodward, A. C. (2011). Experimental Analysis of the Effects of the Variation of Drawbar Pull Test Parameters for Exploration Vehicles on GRC-1 Lunar Soil Simulant. M.S. thesis., Blacksburg, VA: Virginia Tech., Department of Mechanical Engineering.

Zoz, F. M. and Grisso, R.D. (2003). Traction and Tractor Performance. ASAE Distinguished Lecture Series. Tractor Design No. 27.

**For online indexing: Author 1**

| First Name | Middle Name | Surname | Suffix (Jr., etc.) | ORCID (opt.) | Email | Correspondance Author? yes or no |
|---|---|---|---|---|---|---|
| Chetan | M. | Badgujar | | | chetan19@ksu.edu | yes |

**For online indexing: Author 2**

| First Name | Middle Name | Surname | Suffix (Jr., etc.) | ORCID (opt.) | Email | Contact Author? yes or no |
|---|---|---|---|---|---|---|
| Daniel | | Flippo | | | dkflippo@ksu.edu, baldflippo@gmail.com | no |

**For online indexing: Author 3**

| First Name | Middle Name | Surname | Suffix (Jr., etc.) | ORCID (opt.) | Email | Contact Author? yes or no |
|---|---|---|---|---|---|---|
| Edwin | | Brokesh | | | ebrokesh@ksu.edu | no |

**For online indexing: Author 4**

| First Name | Middle Name | Surname | Suffix (Jr., etc.) | ORCID (opt.) | Email | Contact Author? yes or no |
|---|---|---|---|---|---|---|
| Stephen | | Welch | | | welchsm@ksu.ed | no |